

# Separation and identification of trinucleotide–melphalan adducts from enzymatically digested DNA using HPLC–ESI–MS

Dalia Mohamed · Michael Linscheid

Received: 3 April 2008 / Revised: 5 June 2008 / Accepted: 6 June 2008 / Published online: 12 July 2008  
© Springer-Verlag 2008

**Abstract** Melphalan is a bifunctional alkylating agent that covalently binds to the nucleophilic sites present in DNA. In this study we investigated oligonucleotides prepared enzymatically from DNA modified with melphalan. Calf thymus DNA was incubated in-vitro with melphalan and the resulting modifications were enzymatically cleaved by means of benzonase and nuclease S1. Efficient sample pre-concentration was achieved by solid-phase extraction, in which phenyl phase cartridges resulted in better recovery of the modified species than  $C_{18}$ . The applied enzymatic digestion time resulted in production of trinucleotide adducts which were efficiently separated and detected by use of reversed-phase HPLC coupled to an ion-trap mass spectrometer with electrospray ionization. It was assumed that melphalan could act as both a monofunctional and bifunctional alkylating agent. Mono-alkylated adducts were much more abundant, however, and the alkylation site was located on the nucleobases. On the other hand, we unequivocally identified cross-link formation in DNA, even though at low abundance and only a few adduct types were detected.

**Keywords** Melphalan · Nitrogen mustards · DNA adducts · LC–MS–MS · Fragmentation

## Introduction

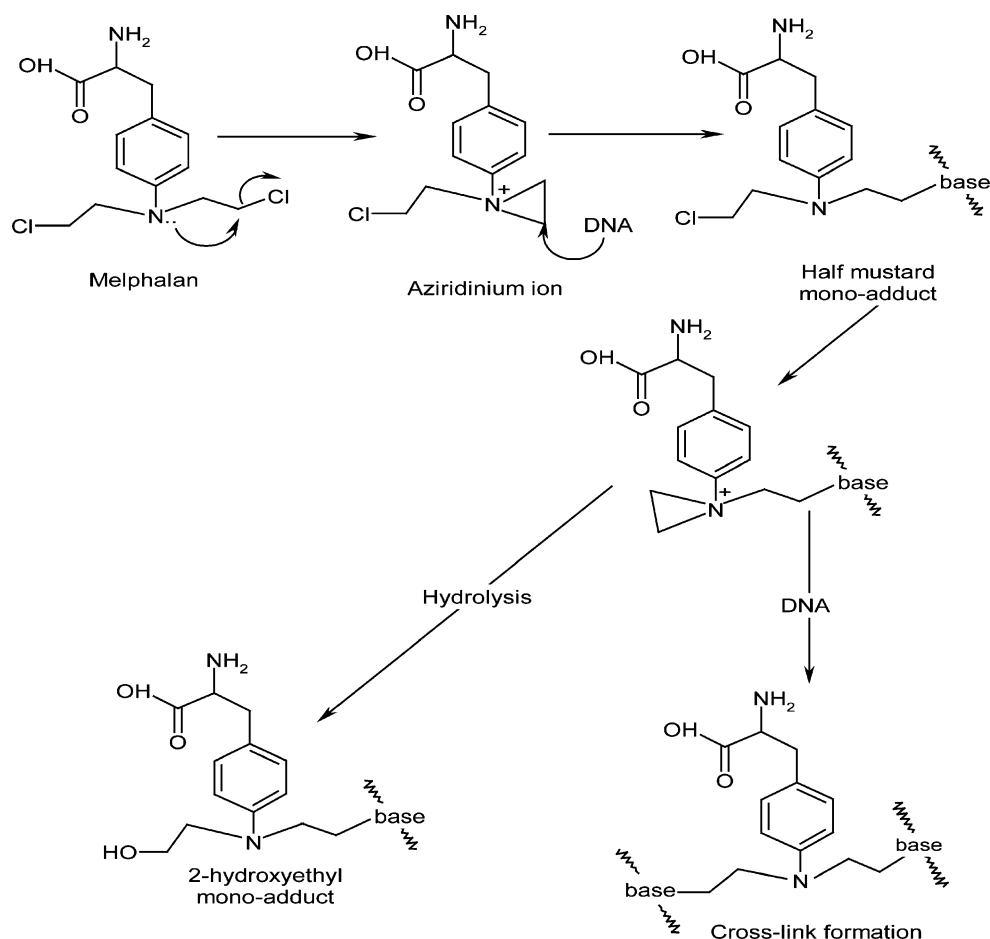
Alkylation of DNA is a key cellular event in the mechanism of action of clinical anticancer drugs, chemical mutagens,

and carcinogens [1, 2]. One of these alkylating agents is the nitrogen mustard (NM) melphalan, currently used in the treatment of malignant melanoma, multiple myeloma, lymphomas and ovarian carcinoma [3]. Melphalan and other therapeutic NMs are known to undergo intramolecular nucleophilic substitution reactions to produce aziridinium ions (Scheme 1) [4]. These reactive intermediates are capable of alkylating multiple sites in DNA, e.g., the N7 of guanine [5], a reaction which has several consequences, such as depurination with strand scission and formation of inter and intrastrand cross-links in addition to alteration of the base structure leading to miscoding [6]. Furthermore, alkylation of the N1, N<sup>6</sup>, N3, and N7 positions of adenine [7–9] has also been observed. Although the 2'-hydroxyethyl derivatives produced by hydrolysis of the second chloroethyl group after initial monoalkylation are the predominant DNA lesions formed as a result of treatment with NM, DNA–DNA cross-links of NM play a critical role in their biological activity [10]. However, Bauer and Povirk [11] have concluded that secondary alkylation of melphalan was much slower than that of other mustards. While mono-adduct formation on the nitrogen atoms or exocyclic oxygens may cause inhibition of DNA replication or base mispairing, the biological impact of DNA–DNA cross-links is strongly dependent on their type. Interstrand cross-link formation is usually associated with cell death or chromosome loss; intrastrand lesions, on the other hand, may be either promutagenic or lethal [8, 10].

Significant effort has been directed toward detection and characterization of melphalan–DNA adducts. Tilby et al. [12, 13] developed immunological assays using an antibody specific for melphalan-alkylated DNA. The same authors have also synthesized a monofunctional derivative of melphalan and have concluded that the level of detectability of cross-linked adducts formed by monohydroxymelphalan

D. Mohamed · M. Linscheid (✉)  
Department of Chemistry, Laboratory of Applied Analytical  
and Environmental Chemistry, Humboldt-Universitaet zu Berlin,  
Brook-Taylor-Str. 2,  
12489 Berlin, Germany  
e-mail: m.linscheid@chemie.hu-berlin.de

**Scheme 1** Aziridinium-ion formation and alkylation reactions observed with melphalan. (Adapted from Ref. [4])



were much lower than those formed by melphalan [14]. Also, melphalan–DNA adducts were detected and quantified at the single cell level in hematopoietic tumor cells [15]. Several approaches were also carried out by Osborne et al. [16, 17] who characterized cross-linked adducts between guanine and adenine and between two guanine residues in DNA. However, the main problem encountered with these methods was the inability to give unambiguous structural information about the detected adducts. Better structural information and sequence identification were obtained by use of electrospray mass spectrometry, and structural characterization can be significantly enhanced when used in combination with MS–MS, i.e. tandem mass spectrometry. Using this technique, Esmans and co-workers were able to analyze melphalan adducts both in calf thymus DNA [18–20] and in in-vivo target organs in the rat [21].

Two analytical approaches based on different techniques have been used for quantitation of melphalan–DNA adducts. Edler et al. [22] used a method depending on the detection of phosphorus using HPLC–inductively coupled plasma mass spectrometry, Van den Driessche et al. [23] have quantified dGuo-melphalan in different tissues from the rat using isotope-dilution mass spectrometry.

In view of the aforesaid, our research aim was to develop a sensitive technique furnishing structural information about melphalan–DNA adducts in the context of neighbor nucleobases by coupling micro-LC to electrospray mass spectrometry. We report on the fragmentation behavior of melphalan trinucleotide adducts of calf thymus DNA observed in the ion trap and then on the specificity of melphalan alkylation with regard to DNA sequence.

## Experimental

### Chemicals and reagents

All solvents were of high-performance liquid chromatography (HPLC) grade. Chemicals were of analytical reagent grade. Melphalan, benzonase enzyme, sodium acetate, and triethylammonium acetate were purchased from Sigma–Aldrich Chemie, Steinheim, Germany. Double-stranded DNA, dimethyl sulfoxide (DMSO), and magnesium acetate were obtained from Merck, Darmstadt, Germany. Calf intestine alkaline phosphatase and nuclease S1 were purchased from Fermentas, St. Leon Rot, Germany. Diethyl

ether and ethyl alcohol were obtained from J.T. Baker, Deventer, The Netherlands. Ammonium acetate was obtained from Riedel–De-Haën, Seelze, Hannover, Germany. The cartridges used for solid-phase extraction were purchased from Varian, Middelburg, NL.

### Sample preparation

DNA adducts of melphalan were prepared by reaction of melphalan with double-stranded DNA. DNA stock solution (4 mg mL<sup>-1</sup> de-ionized water; 250 µL) was incubated with 200 µL melphalan stock solution (1 mg mL<sup>-1</sup> DMSO) and 300 µL DMSO at 37°C for 24 h. Then the reaction mixture was cooled to room temperature and extracted with 750 µL diethyl ether four times. Any excess of diethyl ether was removed in a vacuum centrifuge (SpeedVac AES 1000, Savant Instruments, Farmingdale, NY, USA) for 15 min.

DNA was precipitated with 75 µL 3 mol L<sup>-1</sup> sodium acetate solution (pH 5.2) and 1 mL ice-cold ethanol. The solution was then centrifuged at 4°C and 10,000 g for 15 min using Sigma a 3K30 centrifuge (Sigma Laboratory Centrifuges, Osterode am Harz, Germany). The resulting DNA pellet was washed twice with 100 µL aqueous ethanol (70%) and dried under vacuum.

For enzymatic hydrolysis of DNA, the dried DNA pellet was re-dissolved in 400 µL magnesium acetate solution (2 mmol L<sup>-1</sup>), then 25 units benzonase enzyme were added either alone or followed by 1.75 units calf intestine alkaline phosphatase. The resulting solution was incubated at 37°C for 4 h. Afterwards 600 µL 1× nuclease S1 buffer (pH 4.8) followed by 100 units nuclease S1 enzyme were added, and the solution was further incubated at 37°C for 30 min. Finally, solid-phase extraction (SPE) was carried out for these samples as follows: 1 mL one-way-SPE cartridges filled with 100 mg C<sub>18</sub> or PH sorbent material were used, the cartridges were rinsed successively with 3 mL methanol and 2 mL 10 mmol L<sup>-1</sup> ammonium acetate solution (pH 5) for cleaning and conditioning. After sample absorption, the cartridges were washed with 4 mL ammonium acetate solution to remove unmodified nucleotides and the modified nucleotides were eluted from the cartridges with 2 mL methanol. The solvent was removed in a vacuum centrifuge and the dried residues were re-dissolved in 250 µL ammonium acetate solution (10 mmol L<sup>-1</sup>, pH 5).

### Instrumentation

The chromatographic system consisted of an Ultimate pump (LC Packings, Amsterdam, The Netherlands) using a ULT-MIC-1000 calibrator suitable for column size 0.8–1 mm and a FAMOS (fully automated micro sampling workstation) autosampler (LC Packings) equipped with a 5 µL sample loop, a C<sub>18</sub>, 5-µm particle, 100 Å, 1 mm i.d. × 5 mm

precolumn (LC packings) and a Discovery Bio Wide Pore 1 mm diameter, 10 cm length, 3 µm particle size C<sub>18</sub> chromatographic column (Supelco, Sigma-Aldrich, Germany). The mobile phase was a gradient prepared from 5 mmol L<sup>-1</sup> triethylammonium acetate, pH 5.4 (Eluent A) and 50% 10 mmol L<sup>-1</sup> triethylammonium acetate, pH 5.4, and 50% methanol (Eluent B). Gradient program: 0–5 min 90% A, 5–35 min up to 70% B, 35–40 min 70% B, 40–50 min back to 90% A, 50–60 min equilibration. The flow rate was 50 µL min<sup>-1</sup> and the injected volume was 5 µL.

### Mass spectrometric conditions

Measurements were carried out on an LCQ Deca XP instrument (Finnigan, San Jose, CA, USA) in the negative-ionization mode. The instrument was tuned to the following values: 22 arb nitrogen-sheath gas flow, 4.2 kV sprayer voltage, -33 V capillary voltage, -40 V tube lens offset, 6.75 V multipole 1 offset, 15.5 V multipole 2 offset, 14 V intermultipole lens voltage, 400 V p–p octapole RF amplifier, 66 V entrance lens. The temperature of the transfer capillary was 250°C. In full-scan mode a mass range from 300–1250 was scanned. MS–MS experiments were carried out using an isolation width of  $\Delta m/z$  4, activation amplitude 35%, and activation time 55 ms.

### Results and discussion

Modifications of DNA at the oligonucleotide level caused by melphalan were studied by digesting calf thymus DNA after melphalan incubation for 24 h in a ratio of 1:5 (melphalan:nucleotide). Enzymatic digestion was performed with the aid of benzonase and nuclease S1 (NS1) enzymes. Benzonase, an enzyme developed to purify proteins from nucleic acids by cleaving DNA and RNA unspecifically [24], cleaves the DNA into oligonucleotides with chain lengths of 2–8 nucleobases [25]. Nuclease S1 cleaves phosphodiester bonds on single-stranded DNA [26] and will continue to digest unpaired pairs from the DNA until all single-stranded positions are digested, displaying both endo and exonuclease activity. Variation of the enzymatic digestion time for benzonase (4–24 h) seemed to have little effect on the abundance of the detected adducts. In contrast, NS1 digestion time was very critical in order to digest the majority of modifications to the 2'-deoxytrinucleotides and deoxytrinucleoside diphosphate. Maximum abundance of the required adducts was observed upon decreasing the NS1 digestion time to 30 min; when attempting to use shorter time, however, an undesirable decrease in the abundance of these adducts was observed. One of the main drawbacks of using short NS1 digestion time was the production of large amounts of unmodified

nucleotides, consequently hampering detection of the modified compounds in the electrospray ionization process. It was therefore decided to use solid-phase extraction as the last step in the sample preparation. SPE was very useful not only in removing a part of the native nucleotides but also in pre-concentration of the adducts prior to their analysis. As demonstrated in Fig. 1, phenyl-modified silica-gel cartridges (PH cartridge) led to better results than octadecyl silica-gel cartridges ( $C_{18}$  cartridge). Although  $C_{18}$  is the most hydrophobic silica-based sorbent, and the most popular, because of its great retention capabilities for non-polar compounds, in our context it is regarded as the least selective, because it retains most organic analytes from aqueous matrices. On the other hand PH cartridges exhibit slightly different selectivity from other non-polar sorbents. This added selectivity results from the electron density of the aromatic ring which in turn has led to better recovery for melphalan-containing compounds.

## Fragmentation

### Mono-alkylated 2'-deoxytrinucleotide–melphalan adducts

As described in Scheme 1, the chloroethyl group of the melphalan side-arm can cyclize to form an aziridinium ion; in the following text, the half mustard mono-adduct formed by alkylation of a nucleobase will be referred to as mel(Cl). Following this alkylation, the second chloroethyl group can

react with a water molecule, giving rise to 2-(hydroxyethyl) mono-adducts, mel(OH). Melphalan modification to the trinucleotides was specifically located on the base moieties (G, C, and A) which was very clear from the presence of the characteristic fragment of the alkylated base, i.e. B-mel (OH/Cl) in all MS–MS spectra of the detected adducts, a list of  $m/z$  of these ions is given in Table 1.

These modifications were detected either as singly or doubly charged species (Fig. 2). The fragmentation nomenclature used was that developed by McLuckey and Habibi-Goudarzi [27].

Modified trinucleotides possessing guanosine moieties were detected mainly as doubly charged species where the singly charged ones were of low abundance. Two main types of modified sequence were detected and we assigned these to  $G^*NN$  and  $NG^*N$  (\* indicates the position of alkylation). On the other hand, no signal was observed for the  $NNG^*$  sequence, whose absence was probably a result of the enzymatic action. It became apparent that the enzymes used were incapable of digesting the oligomers when the site of alkylation is on the 3' end of the sequence.

A single specific fragmentation pathway was evident upon activation of the trinucleotide and the trinucleoside diphosphate guanine adducts (Fig. 3). Cleavage of the *N*-glycosidic bond of the alkylated guanine yielded two major negatively charged complementary ions—the alkylated base and the depurinated backbone. Subsequent cleavage of the ribose 3' C–O bond adjacent to the G alkylation site was

**Fig. 1** Base peak ion chromatograms ( $m/z$  550–650) of the digested DNA–melphalan samples using different cartridges during SPE: a,  $C_{18}$  cartridges; b, PH cartridges

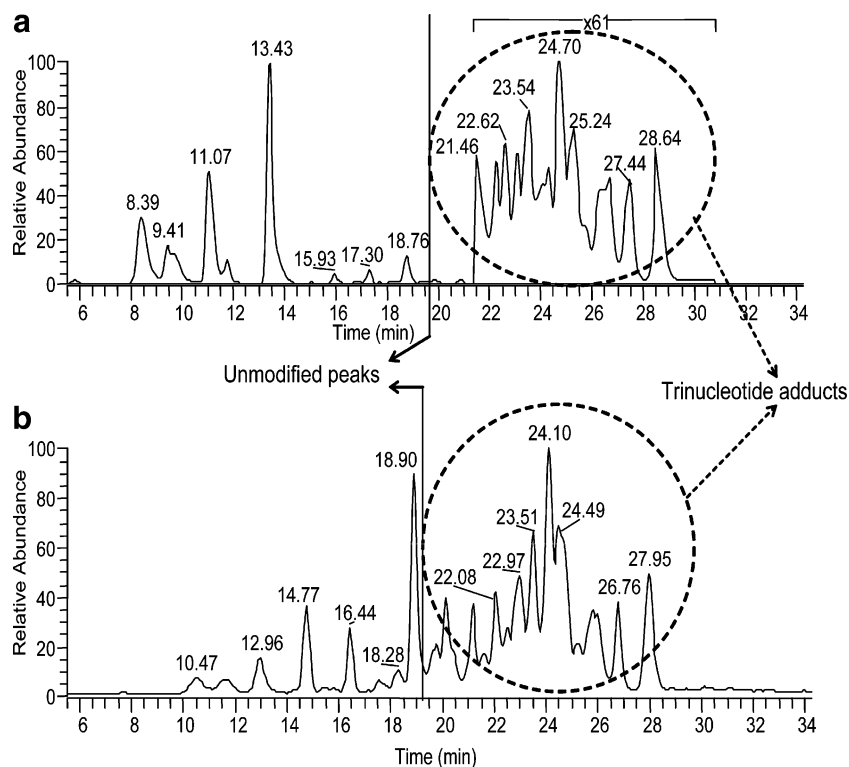


**Table 1**  $m/z$  of the alkylated base fragments with both mel(OH) and mel(Cl)

Base	$m/z$	
	mel(OH)	mel(Cl)
Adenine	384	402
Cytosine	360	378
Guanine	400	418

more informative, because it gave rise to either an unmodified  $w_2^-$  ion for the adducts belonging to the G\*NN sequence (Scheme 2) or the two alternative negatively charged fragments—unmodified  $w_1^-$  and modified  $(a_2 - B_2)^-$  for adducts possessing the NG\*N sequence. It was evident that the  $(a_2 - B_2)^-$  ion was generated in higher abundance than the  $w_1^-$  ion, a possible explanation might be related to the charge distribution on the phosphate residues. Being more electronegative,  $(a_2 - B_2)^-$  was more capable of possessing the charge and so was more likely to be produced.

This type of specific fragmentation was reported previously in negative-ion MS–MS spectra of adducts formed between hedamycin (a naturally occurring intercalating alkylating agent) and the oligonucleotide 5'-CACGTG-3' [28].

On the other hand several singly and doubly charged species involving alkylation to adenine and cytosine were detected. Although melphalan alkylation of cytosine base

has given rise to both C\*N\*NN and NC\*N types of sequence, all the detected adenine adducts belonged to the A\*NN sequence only. Generally most of the extracted single mass chromatograms corresponding to the doubly charged adenine adducts showed low peak intensity and low signal-to-noise ratio. Specifically this feature was more apparent upon comparing the abundance of the alkylated adenine and cytosine isomers, as shown in Fig. 4.

Modified species involving cytosine and adenine alkylation showed similar fragmentation behavior in the ion trap. With regard to the doubly charged trinucleotide species, a major fragment corresponding to  $PO_3^-$  loss was detected with 100% relative abundance in all MS<sup>2</sup> spectra. This direct loss from the parent ion is commonly observed for oligomers phosphorylated at the 5' sugar and competes with the major fragmentation channels. In addition this loss affects the abundance of the other sequence specific ions. Nevertheless, these ions were still detectable and complete sequence information could be obtained from the 1st-generation product ions only. The ions of the w-series, the a-series and  $(a_2 - B_2)^-$  ions were observed. The position of the alkylation was identified based on the sequence-specific fragments possessing the melphalan side chain as displayed in Fig. 5a.

For the singly charged species (Fig. 5b) elimination of water and neutral loss of the unmodified 5' base are other major fragmentation pathways replacing the  $PO_3^-$  loss observed in the doubly charged species. Beside the

**Fig. 2** Mass spectra of melphalan–trinucleotide adducts produced after incubation of DNA with melphalan for 24 h followed by digestion with benzonase (4 h) and nuclease S1 (30 min): a, doubly charged species ( $m/z$  550–650); b, singly charged species ( $m/z$  1100–1250)

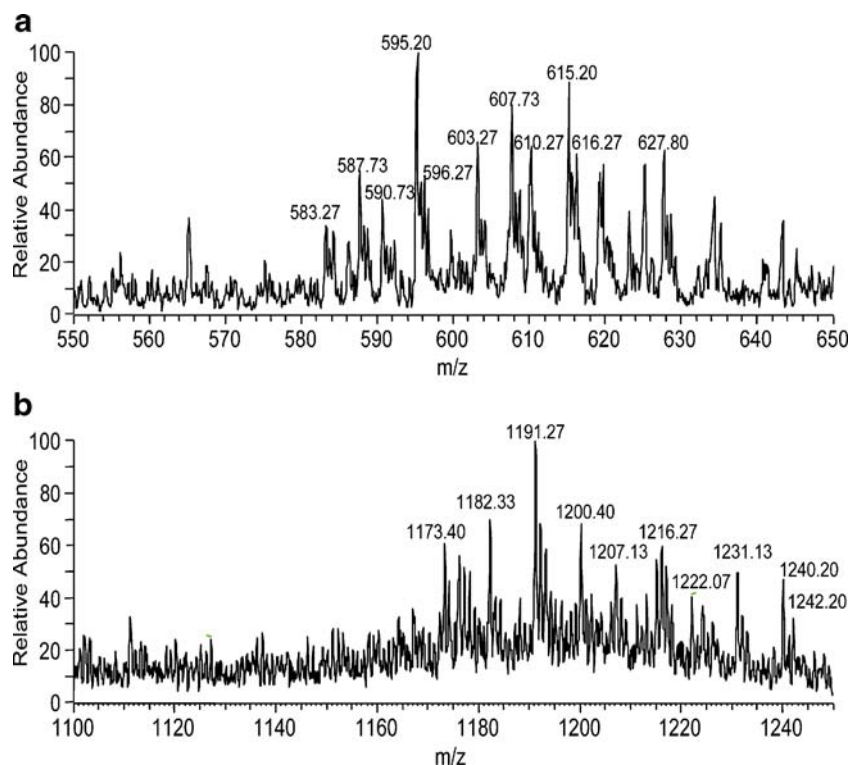
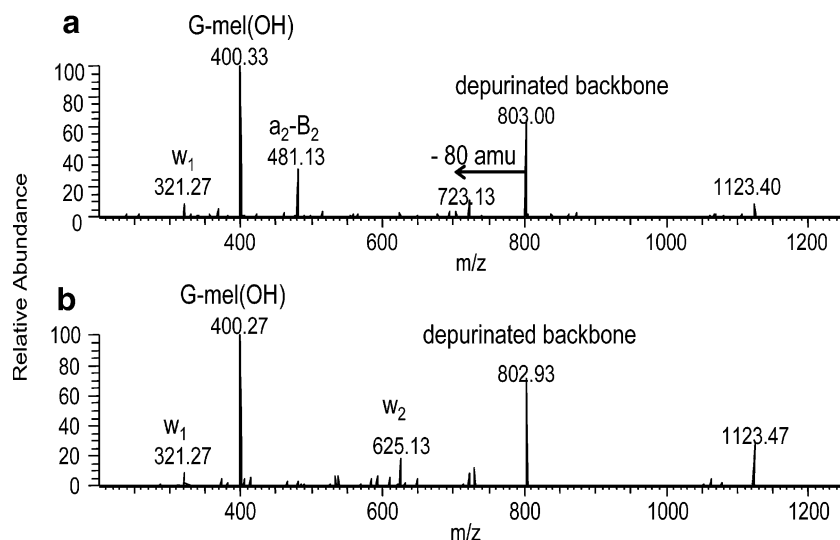


**Fig. 3** MS<sup>2</sup> spectra of [M - 2H]<sup>2-</sup> at m/z 601.7: a, pd (TG\*T)-mel(OH); b, pd (G\*TT)-mel(OH)



sequence-specific fragments discussed previously, a few low-abundance fragments were detected such as the modified  $d_2^-$  ion, whose proposed mechanism of formation involves cleavage of the 5'-phosphate di-ester linkage accompanied by proton transfer from the ribosyl group to the phosphate moiety, which occurs through a favorable six-membered cyclic transition state [29]. The  $z_2$  ion might arise via elimination of the 5' terminus base followed by proton transfer. This can subsequently trigger cleavage of the CH<sub>2</sub>-O bond at the 5' end to give an ion-molecule

complex between the  $(d_1 - B_1)^-$  ion and the  $z_2$  neutral species, which could ultimately yield the  $z_2^-$  ion and the neutral  $(d_1 - B_1)$  molecule via proton transfer [30], in addition to the  $b_2^-$  ion, which was probably produced via a direct cleavage of the P-O bond from the deprotonated parent ion resulting in charge transfer to the 5' end of the molecule.

With regard to the fragmentation behavior of the cytosine and adenine trinucleoside diphosphate adducts, it seems that loss of the 5' base, either modified or unmod-

**Scheme 2** Characteristic collision-induced MS-MS fragments from the doubly charged G\*NN sequence (G\* is the guanine with the melphalan chain). The charge location is only tentative

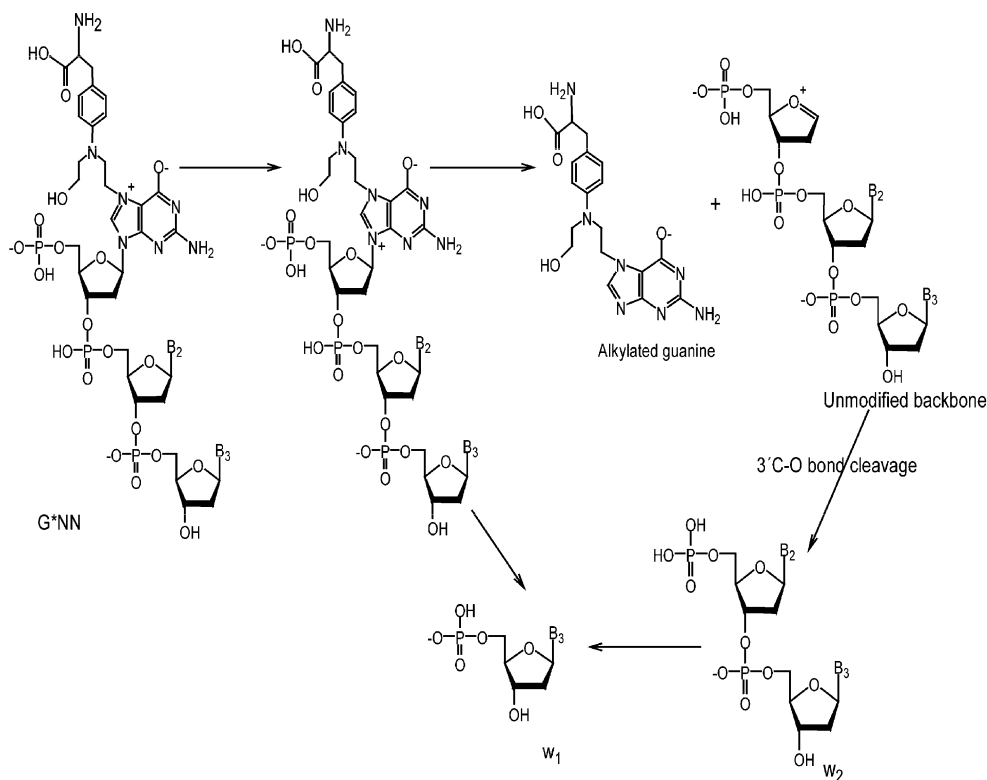


**Fig. 4** Extracted single mass chromatograms showing peak area and *S/N* ratio for the doubly charged adducts: a, *m/z* 595.5; b, *m/z* 590.5

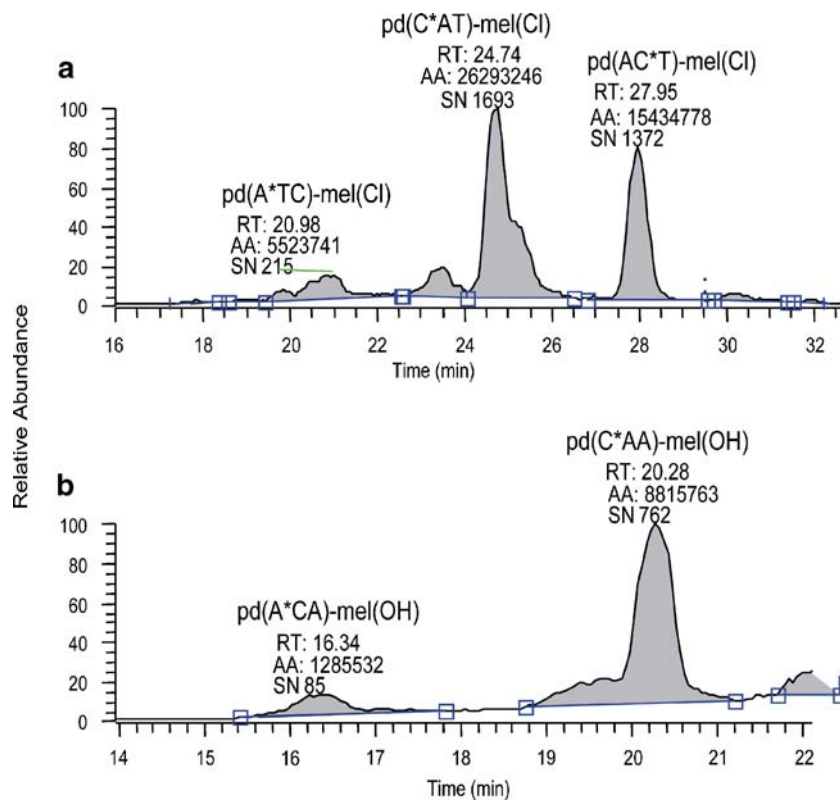


**Fig. 5** MS–MS spectra of (a) doubly charged pd(TC\*T)-mel(OH) *m/z* 581.7 and (b) singly charged pd(TC\*T)-mel(OH) *m/z* 1164. (Fragments carrying the modification are assigned with an asterisk)

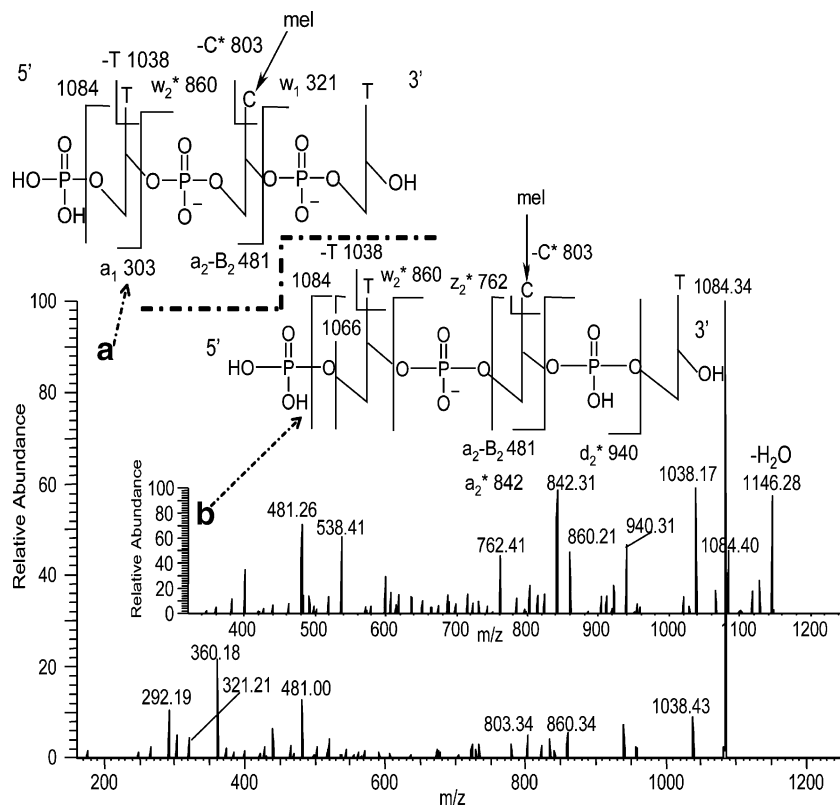
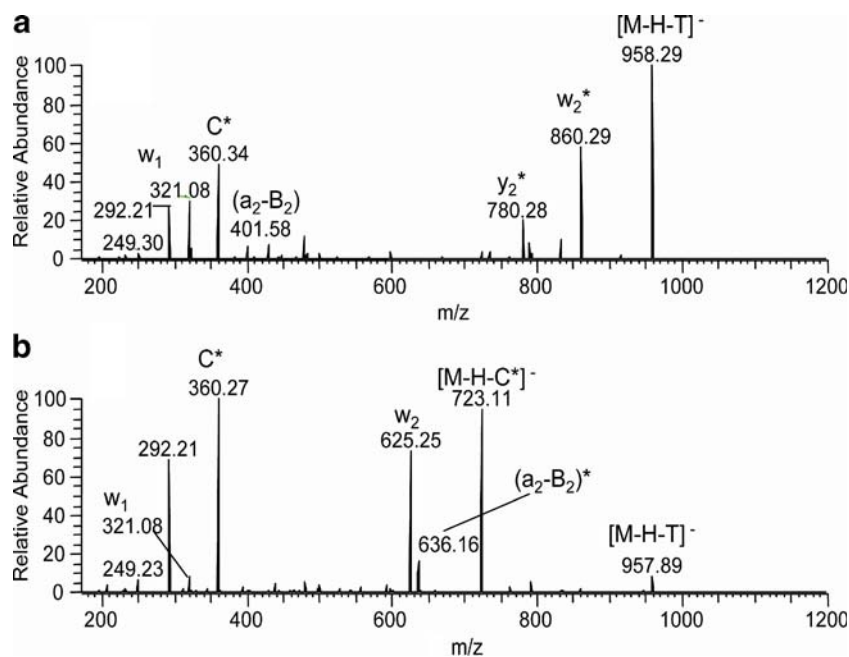


**Fig. 6** MS–MS spectra of the doubly charged adduct at  $m/z$  541.8: a, d(TC\*T)-mel(OH); b, d(C\*TT)-mel(OH)



ified, followed by the 3' C–O bond break was the major reaction (Fig. 6). This explanation is based on detection of the ions corresponding to  $[M - H - B_1]^-$  and  $w_2^-$  with relatively high abundance. In a minor fragmentation pathway,  $B_2$  might also be lost followed by strand cleavage leading alternatively to  $(a_2 - B_2)^-$  and  $w_1^-$  ions. Cleavage of the P–O bond was observed in the NC\*N group of adducts, resulting in the production of the  $y_2^-$  fragment. We should point to the absence of this fragment for the trinucleotide adducts, which means that the presence of the 5' phosphate moiety affects this pathway.

More fragments of all the detected adducts are listed in Table 2. An examination of the data presented in this table revealed that both non-sequence and sequence ions were formed. The former consist of the ions resulting from base loss in the order  $A > T > G > C$ , which is in agreement with results reported by McLuckey [27], Beauchamp [29], and O'Hair [30]. The latter were dominated by abundant  $w_1^-$ ,  $w_2^-$ , and  $(a_2 - B_2)^-$ , with minor  $a_1^-$  and  $a_2^-$  ions.

It has been shown that ionization efficiencies for nucleotides having the same number of phosphates are very similar [31, 32], thus we could get some information about sequence preferences based on peak-area measurement for the adducts. As demonstrated in Table 2, the sequences detected in higher abundances were those possessing a thymine base on the 3' terminus. Then adenine or thymine were usually located either in the 5' terminus (i.e. (T/A)N\*T) or in the middle position of the sequence (i.e. N\*(A/T)T), with the exception of G\*CT which was of moderate abundance only. So we found C\*AT-mel(Cl) as

the most abundant adduct. This is in agreement with data from DNA digested to dinucleotides, where we found C\*A as the most abundant species (data not included). In order to ensure the reproducibility of the results obtained, the experiments were repeated several times over a long period, where these results proved to be reproducible in terms of sequence distribution and intensities. In a study by Van den Driessche et al. [33] on the interaction of melphalan and 2'-oligodeoxynucleotides, it was concluded that melphalan alkylation occurs in the sequence  $G > A > C > T$ . Nearly similar results were obtained by us on investigating the reaction between melphalan and some synthetic tetranucleotides, where also guanine was the most preferential site for melphalan alkylation. However, the observed differences in the alkylation order for the bases from the digested DNA samples could be explained by the incubation and digestion time. Most of the guanine adducts were lost by the well-known depurination reaction, which occurs when N7 of guanine is alkylated. In addition, the presence of some guanine deglycosylation products in the reaction mixture could be put forward as evidence in favor of this explanation.

#### Cross-linked adducts

The ability of melphalan to cross-link DNA is attributed to the presence of two electrophilic centers in its molecule. Both of the 2-(chloroethyl) groups may cyclize to an aziridinium ion, consequently alkylating two nucleobases within the DNA duplex.

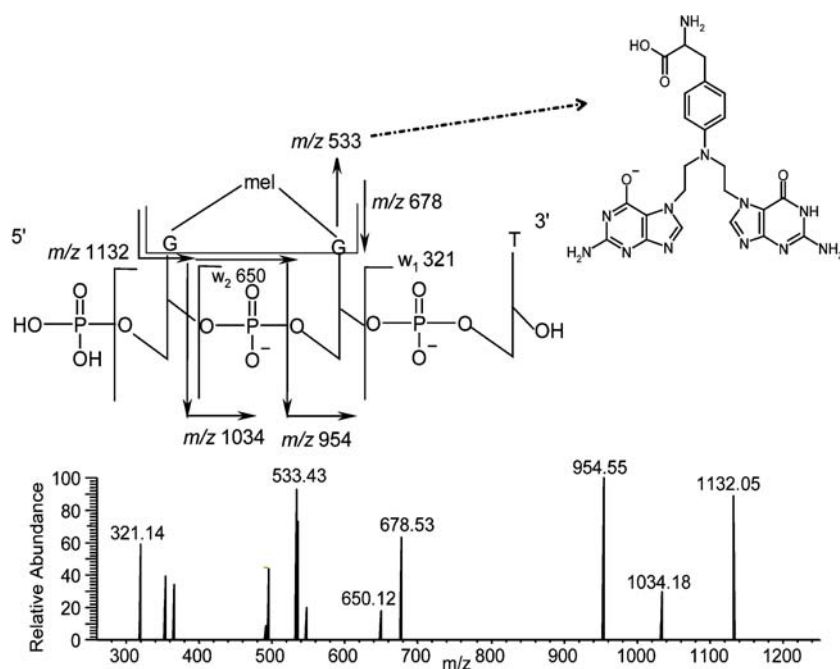


**Table 2** CID MS–MS of the  $[M - 2H]^{2-}$  ions of all detected trinucleotide adducts

pd(B <sub>1</sub> B <sub>2</sub> B <sub>3</sub> ) <i>m/z</i> value <sup>a</sup>	<i>t<sub>r</sub></i> (min)	Product ions (percentage relative abundance)									RPA <sup>b</sup>
		w <sub>1</sub> <sup>-</sup>	w <sub>2</sub> <sup>-</sup>	a <sub>1</sub> <sup>-</sup>	a <sub>2</sub> <sup>-</sup>	(a <sub>2</sub> - B <sub>2</sub> ) <sup>-</sup>	- PO <sub>3</sub> <sup>-</sup>	alk base	- alk base	- base	
Alkylation with mel(OH)											
C*TC(574)	19.89	4	12	–	–	15	100	34	20	T 8	0.12
CC*T(574)	21.43	4	17	4	3	18	100	26	14	T 5	0.27
C*AC(578.8)	18.83	24	10	22	4	30	100	15	8	A 20	0.10
AC*C(578.8)	19.52	4	6	8	5	22	100	48	22	A 26	0.35
C*TT(581.7)	21.72	8	18	8	5	12	100	12	24	T 6	0.40
TC*T(581.7)	22.40	8	12	5	–	24	100	38	24	T 10	0.42
C*AT(586)	20.30	20	20	7	5	46	100	16	10	A 16	0.61
AC*T(586)	24.04	8	20	5	–	14	100	16	10	A 20	0.41
C*AA(590.5)	20.11	12	10	15	12	30	100	18	10	A 26	0.42
GC*T(594)	21.93	15	25	7	–	10	100	10	7	–	0.35
A*CA(590.5)	16.11	8	10	8	5	18	100	12	5	A 15	0.06
A*AC(590.5)	15.28	5	10	8	12	18	100	12	5	A 20	0.06
A*TT(593.5)	18.32	10	15	15	–	10	100	30	10	T 5	0.17
A*AA(602.5)	15.92	12	15	9	–	25	100	7	25	A 30	0.14
A*GT(606.2)	20.80	7	12	5	–	20	100	10	10	G 10	0.23
G*CT(594)	18.32	5	40	–	–	–	10	95	100	–	0.51
TG*T(601.7)	19.53	7	–	–	–	40	10	100	70	–	0.43
G*TT(601.7)	21.01	5	20	–	–	–	30	100	80	–	0.52
G*AT(606.2)	19.83	5	20	–	–	–	20	100	90	–	0.30
AG*T(606.2)	20.33	5	–	–	–	30	15	100	70	–	0.46
G*AA(610.5)	18.96	5	25	–	–	–	10	100	90	–	0.25
AG*A(610.5)	19.78	7	–	–	–	30	10	100	40	–	0.41
Alkylation with mel(Cl)											
C*CC(576)	20.99	12	43	10	15	12	100	11	10	–	0.24
C*TT(591)	25.60	8	12	8	5	15	100	10	10	T 8	0.66
TC*T(591)	26.39	5	10	5	5	16	100	12	10	T 10	0.65
C*AT(595.5)	24.74	14	10	5	–	26	100	12	10	A 12	1.00
AC*T(595.5)	27.95	5	12	5	–	15	100	10	13	A 15	0.64
C*GA(608)	21.72	20	10	5	–	35	100	12	5	A 10	0.16
A*TC(595.5)	20.66	7	15	8	–	17	100	9	7	–	0.36
A*TT(603)	22.21	5	10	10	–	10	100	7	20	T 5	0.59
A*AT(607.5)	21.42	20	10	10	–	25	100	10	10	A 20	0.53
A*AA(612)	20.70	10	7	–	–	20	100	7	10	A15	0.08
A*GT(615.5)	20.98	5	15	–	–	20	100	7	15	–	0.10
A*GG(628)	21.82	7	10	–	9	15	100	25	12	–	0.05
TG*C(603.5)	22.62	5	–	–	–	40	60	100	90	–	0.14
G*CT(603.5)	23.59	10	50	–	–	–	40	85	100	–	0.31
G*CA(608)	23.50	5	20	–	–	–	20	85	100	–	0.14
G*AC(608)	24.56	5	15	–	–	–	10	90	100	–	0.13
TG*T(611)	24.94	12	–	–	–	40	20	95	100	–	0.61
G*TT(611)	26.41	20	30	–	–	–	20	90	100	–	0.57
AG*T(615.5)	24.70	12	–	–	–	25	10	100	90	–	0.58
G*AT(615.5)	25.04	6	15	–	–	–	15	100	75	–	0.63
GG*T(623.5)	23.74	7	–	–	–	25	20	100	85	–	0.30
G*GT(623.5)	24.31	7	40	–	–	–	20	100	80	–	0.20
GG*A(628)	23.50	5	–	–	–	20	26	90	100	–	0.10

<sup>a</sup> The position of modification is assigned with an asterisk<sup>b</sup> Relative peak area measured as an average from three experiments

**Fig. 7** MS<sup>2</sup> spectrum of the doubly charged pd(G<sup>^</sup>GT)–mel at *m/z* 605.7



Doubly charged intrastrand cross-linked adducts pd(G<sup>^</sup>GT)–mel *m/z* 605.7 (I), pd(GG<sup>^</sup>A)–mel *m/z* 609.5 (II), and d(G<sup>^</sup>CA)–mel *m/z* 549.8 (III)

The absence of the alkylated base fragment and the presence of the cross-linked fragments G–mel–G (*m/z* 533), G–mel–A (*m/z* 517), and G–mel–C (*m/z* 493) with

the complementary ions at *m/z* 678, *m/z* 702, and *m/z* 606 in the CID spectra of adducts I, II, and III, respectively, has pointed to the possibility of cross-link formation. A characteristic feature in the MS–MS spectrum of I was the loss of neutrals from the 5' end of the sequence where the 5' guanine was still linked to the backbone through melphalan (Fig. 7). In addition, the presence of *m/z* 321 d(TMP) was

**Fig. 8** (a) MS<sup>3</sup> spectrum of *m/z* 533 (G–mel–G) and (b) MS<sup>4</sup> spectrum of *m/z* 490 (G–mel–G#). The structures are tentative and only meant to rationalize the elemental composition assumed from the fragmentation

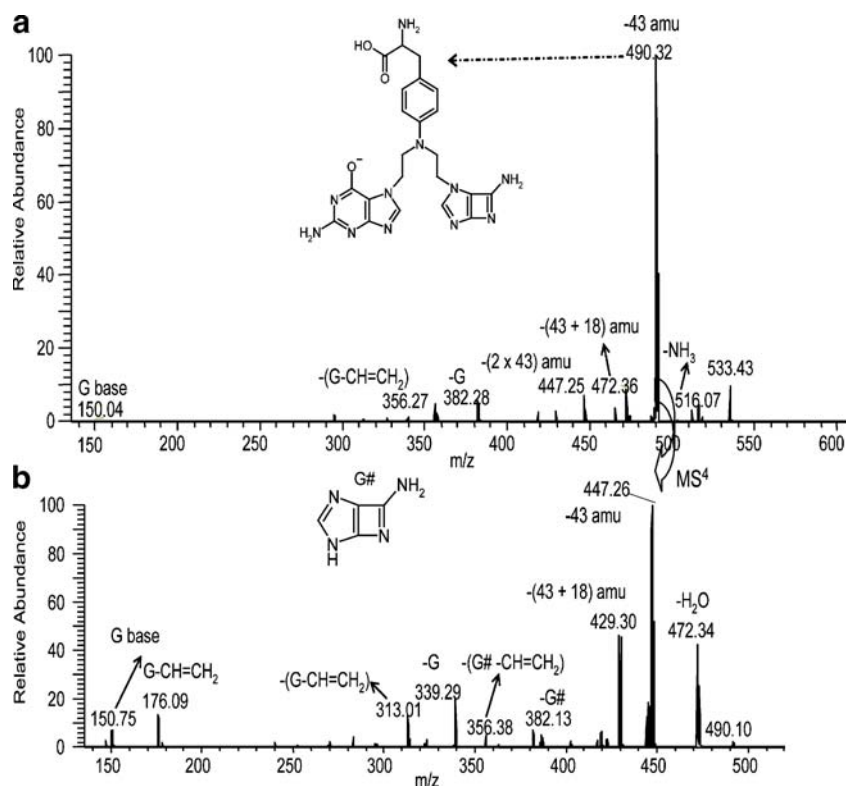
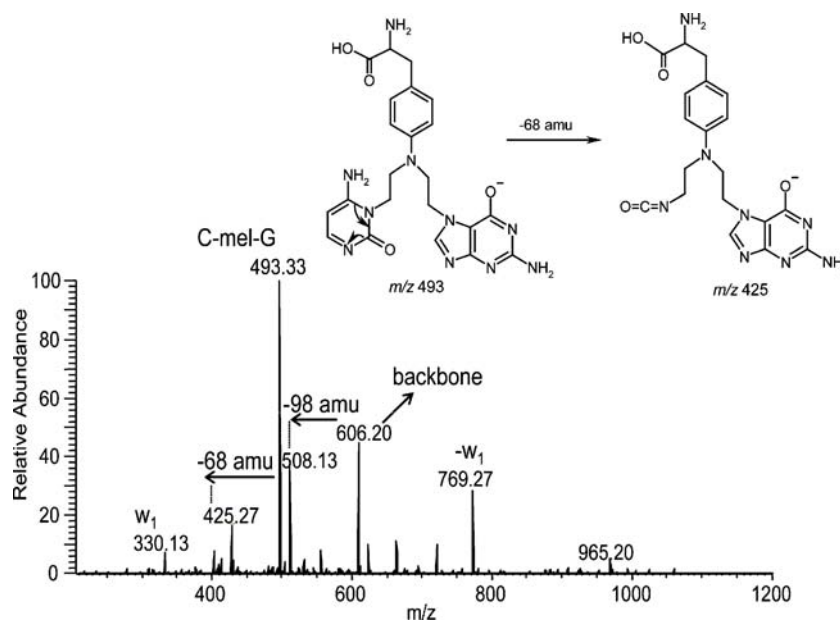


**Fig. 9** MS–MS spectrum of the doubly charged d(G<sup>^</sup>CA)–mel at  $m/z$  549.8. The elimination of C<sub>3</sub>H<sub>4</sub>N<sub>2</sub> is shown indicating the N3 position as alkylation site



useful to identify the sequence. In order to establish the structural assignment of adduct I to a cross-linked adduct, MS<sup>n</sup> experiments were carried out specifically for the characteristic ion at  $m/z$  533 (G–mel–G; Fig. 8). Typical guanine fragmentation—HNCO split via a retro-Diels–Alder reaction (RDA) [34]—was observed. In addition, detection of  $m/z$  176 (G–CH = CH<sub>2</sub>) gave evidence that the guanine base carried a modified chain.

The low abundance of the unmodified backbone in the fragmentation spectrum of adduct II prevented full sequence information from being obtained; however, the absence of the  $w_1$  fragment points towards an unbound guanine at the 5' position.

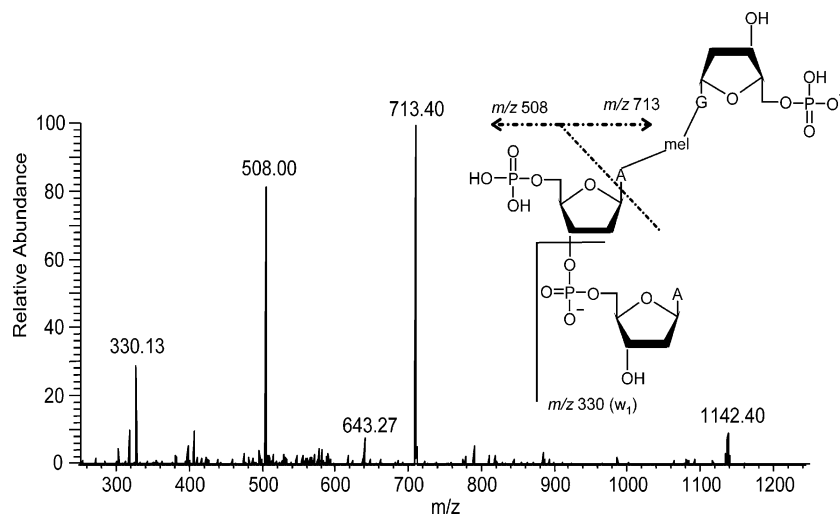
The loss of the cross-linked bases as a first step in the fragmentation of adducts III obscured the position of guanine and cytosine bases in the sequence (Fig. 9). So two structures are possible for this compound—either d

(G<sup>^</sup>CA)–mel or d(C<sup>^</sup>GA)–mel, where the 3' position should be occupied by adenine (presence of  $m/z$  330). A very informative ion appeared at  $m/z$  425. This ion was generated via elimination of 68 amu from  $m/z$  493 and we assumed fragmentation of cytosine in an RDA-type reaction. In the fragmentation spectra of all cytosine adducts, the fragment at  $m/z$  360 (alkylated cytosine) was accompanied by  $m/z$  292, which is again the loss of 68 amu as proven by MS<sup>n</sup> experiments. This characteristic loss pinpoints the alkylation at the N3 position of the cytosine.

Doubly charged interstrand cross-linked adduct d (G\*MP)–mel–pd(A\*A)  $m/z$  610.7

This adduct is an example of an melphalan interstrand cross-linked adduct occurring between a mononucleotide d (GMP) and a dinucleotide pd(AA). The major fragmenta-

**Fig. 10** MS<sup>2</sup> spectrum of the doubly charged d(G\*MP)–mel–pd(A\*A) at  $m/z$  610.7



tion route resulted from the depurination of the bound adenine base, consequently leading to the production of the two complementary ions the unmodified backbone at  $m/z$  508 (pdpdA) and the cross-linked fragment at  $m/z$  713 (d(G\*MP)–mel–A; Fig. 10). The main fragment produced from MS<sup>3</sup> of the latter ion corresponds to adenine loss, which was indicative of the presence of guanine on the mononucleotide side, while 3' C–O bond break of the former ion gives rise to the unmodified  $w_1^-$  ion at  $m/z$  330, pointing to the alignment of the unbound adenine to the 3' terminus of the dinucleotide. In addition, the presence of the unmodified dinucleotide pd(AA) at  $m/z$  643 in the MS–MS spectrum, although at low abundance, can be regarded as additional proof for the structural assignment. Last, the ion at  $m/z$  1142 corresponded to elimination of  $PO_3^-$  from the parent adduct.

Despite detection of the previously mentioned cross-linked adducts with relatively low abundance, specifically when compared with the mono-alkylated adducts, it was of important significance. It is well known that the cytotoxic and anticancer activity of nitrogen mustards closely correlates with the formation of DNA–DNA cross-links. These bifunctional lesions are capable of blocking DNA replication and transcription, eventually leading to cell death and the inhibition of tumor growth [35, 36].

## Conclusion

In this study we used a combination of the enzymes benzonase and nuclease S1, to digest melphalan-modified DNA into trinucleotides by carefully controlling the digestion time. In addition we have solved the problem of separating the vast amount of unmodified nucleotides from the modified oligonucleotides of interest and improving the recovery by the correct choice of the adsorbing material in solid-phase extraction. The developed HPLC–ESI MS method provides sufficient separation of the adducts, and peaks in the mass range 550–650 Da have been assigned to adduct structures. Tandem mass spectrometry was used successfully for structural characterization of melphalan–DNA modifications, specifically for the mono-alkylated adducts. In addition the structures of two cross-linked adducts were elucidated; these corresponded to d(G\*MP)–mel–pd(A\*A) and pd(G^GT)–mel–inter and intrastrand cross-linked adducts, respectively. Thus, there is no doubt that even under very mild enzymatic conditions cross-links can be found, in contradiction of previous results [37].

With regard to the different fragmentation behavior, the doubly charged guanine adducts of the trinucleotides were characterized by a single major fragmentation pathway beginning with depurination of the alkylated guanine base followed by 3' C–O bond cleavage. Doubly charged

adenine and cytosine trinucleotide adducts followed the rules of fragmentation developed for the native nucleotides by McLuckey and Habibi–Goudarzi [27], and by recognizing the sequence-specific fragments possessing the melphalan side chain it was straightforward to identify the sequence. However, fragmentation spectra of singly charged species are more complex and show, beside the predominant ions of the w-series and a-series, several atypical ions, for example  $b_2^-$ ,  $z_2^-$ , and  $d_2^-$ .

Based on the abundance of the detected adducts we conclude that there was a preference for triplets with a thymine specifically at the 3' terminus. Then adenine or thymine were usually located either in the 5' or in the middle position of the sequence.

Future work with other alkylating agents, especially chlorambucil will give us the opportunity to compare the specificity of alkylation of different drugs with regard to DNA sequence and to investigate cross-link formation in further detail.

**Acknowledgements** We are grateful to the Arab Republic of Egypt for a grant to D.M. and to the DFG for financial support of M.L.; Stefan Pieper's expert technical assistance with the mass spectrometers is also gratefully acknowledged.

## References

- Blackburn GM, Gait MJ (1990) Nucleic acids in chemistry and biology. IRL Press at Oxford University Press, UK
- Wilman DEV (1990) The chemistry of antitumor agents. Blackie, Glasgow, UK
- Furner RL, Brown RK (1980) Cancer Treat Rep 64:559–574
- Povirk LF, Shuker DE (1994) Mutat Res 318:205–226
- Osborne MR, Lawley PD (1992) Chem Biol Interact 84:189–198
- Blackburn GM, Gait MJ (1996) Biological consequences of DNA alkylation. In: Nucleic acids in chemistry and biology. Oxford University Press, Hong Kong
- Hemminki K, Kallama S (1986) IARC Sci Publ 78:55–70
- Balcome S, Park S, Quirk Dorr DR, Hafner L, Phillips L, Tretyakova N (2004) Chem Res Toxicol 17:950–962
- Wang P, Bauer GB, Bennett RAO, Povirk LF (1991) Biochemistry 30:11515–11521
- Rajski SR, Williams RM (1998) Chem Rev 98:2723–2796
- Bauer GB, Povirk LF (1997) Nucleic Acids Res 25:1211–1218
- Tilby MJ, Lawley PD, Farmer PB (1990) Chem Biol Interact 73:183–194
- Tilby MJ, McCartney H, Cordell J, Frank AJ, Dean CJ (1995) Carcinogenesis 16:1895–1901
- Tilby MJ, McCartney H, Gould KA, O'Hare CC, Hartley JA, Hall AG, Golding BT, Lawley PD (1998) Chem Res Toxicol 11:1162–1168
- Frank AJ, Proctor SJ, Tilby MJ (1996) Blood 88:977–984
- Osborne MR, Lawley PD (1993) Chem Biol Interact 89:49–60
- Osborne MR, Lawley PD, Crofton-Sleigh C, Warren W (1995) Chem Biol Interact 97:287–296
- Hoes I, Lemiere F, Van Dongen W, Vanhoutte K, Esmans EL, Van Bockstaele D, Berneman Z, Deforce D, Van den Eeckhout EG (1999) J Chromatogr B 736:43–59
- Hoes I, Van Dongen W, Lemiere F, Esmans EL, Van Bockstaele D, Berneman ZN (2000) J Chromatogr B 748:197–212

20. Van den Driessche B, Lemièrè F, Van Dongen W, Esmans EL (2003) *J Chromatogr B* 785:21–37
21. Van den Driessche B, Lemièrè F, Van Dongen W, Van der Linden A, Esmans EL (2004) *J Mass Spectrom* 39:29–37
22. Edler M, Jakubowski N, Linscheid M (2006) *J Mass Spectrom* 41:507–516
23. Van den Driessche B, Esmans EL, Van der Linden A, Van Dongen W, Schaerlaken E, Lemièrè F, Witters E, Berneman Z (2005) *Rapid Commun Mass Spectrom* 19:1999–2004
24. Schrader W, Linscheid M (1997) *Arch Toxicol* 71:588–595
25. Janning P, Schrader W, Linscheid M (1994) *Rapid Commun Mass Spectrom* 8:1035–1040
26. Bartolini WP, Bentzley CM, Johnston MV, Larsen BS (1999) *J Am Soc Mass Spectrom* 10:521–528
27. Mcluckey SA, Habibigoudarzi S (1993) *J Am Chem Soc* 115:12085–12095
28. Iannitti P, Sheil MM, Wickham G (1997) *J Am Chem Soc* 119:1490–1491
29. Rodgers MT, Campbell S, Marzluff EM, Beauchamp JL (1994) *Inter J Mass Spectrom Ion Proc* 137:121–149
30. Vrkic AK, O’Hair R AJ, Foote S (2000) *Aust J Chem* 53:307–319
31. Siethoff C, Feldmann I, Jakubowski N, Linscheid M (1999) *J Mass Spectrom* 34:421–426
32. Liao Q, Chiu NH, Shen C, Chen Y, Vouros P (2007) *Anal Chem* 79:1907–1917
33. Van den Driessche B, Lemièrè F, van Dongen W, Esmans EL (2004) *J Am Soc Mass Spectrom* 15:568–579
34. Neri N, Sindona G, Uccella N (1983) *Gazz Chim Ital* 113:197–202
35. Lawley PD, Brookes P (1965) *Nature* 206:480–483
36. Lawley PD, Brookes P (1967) *J Mol Biol* 25:143–160
37. Van den Driessche B, Lemièrè F, Witters E, Van Dongen W, Esmans EL (2005) *Rapid Commun Mass Spectrom* 19:449–454